Computers in Biology and Medicine 203 (2026) 111473

Contents lists available at ScienceDirect

Computers in Biology and Medicine

journal homepage: www.elsevier.com/locate/compbiomed

Amplitude symbolic analysis: a tool for the evaluation of the autonomic function complementary to traditional symbolic approach

Alberto Porta [a,b,*], Beatrice Cairo [a], Vlasta Bari [a,b], Chiara Arduino [b], Ilaria Burzo [b], Beatrice De Maria [c], Paolo Castiglioni [d,e], Luc Quintin [f], Aparecida Maria Catai [g], Franca Barbic [h,i], Raffaello Furlan [h,i]

[a] Department of Biomedical Sciences for Health, University of Milan, Milan, Italy
[b] Department of Cardiothoracic, Vascular Anesthesia and Intensive Care, IRCCS Policlinico San Donato, San Donato Milanese, Milan, Italy
[c] Istituti Clinici Scientifici Maugeri IRCCS, Milan, Italy
[d] Department of Biotechnology and Life Sciences, University of Insubria, Varese, Italy
[e] IRCCS Fondazione don Carlo Gnocchi, Milan, Italy
[f] Hopital d'Instruction des Armées Desgenettes, University of Lyon, Lyon, France
[g] Department of Physical Therapy, Federal University of São Carlos, São Carlos, Brazil
[h] Department of Biomedical Sciences, Humanitas University, Pieve Emanuele, Milan, Italy
[i] IRCCS Humanitas Clinical and Research Center, Rozzano, Italy

ARTICLE INFO

Keywords:
Heart rate variability
Symbolic dynamics
Cardiac control
Autonomic nervous system
Pharmacological blockade
Head-up tilt
Parkinson disease

ABSTRACT

Symbolic analysis (SA) infers cardiac control from spontaneous stationary sequences of heart period (HP) by estimating the probability of symbolic pattern classes. Unfortunately, SA does not assess the fraction of HP variability associated with symbolic pattern families. This study proposes amplitude SA (ASA) accounting for absolute changes between consecutive HPs. ASA leverages uniform 6-bin quantization to symbolize HP, the delay embedding procedure to form length-3 symbolic patterns and a traditional strategy to group symbolic patterns into four classes families according to number and sign of variations between adjacent symbols. ASA computes the fraction of variance associated with symbolic pattern classes. ASA was applied to HP variability derived from: 1) healthy subjects during pharmacological challenges (n = 9; age: 25–46 yrs, 9 males); 2) healthy subjects during graded postural stimuli (n = 19; age: 21–48 yrs, 8 males); 3) Parkinson disease (PD) patients (n = 12; age: 55–79 yrs, 8 males) and matched healthy controls (n = 12; age: 58–72 yrs, 7 males). We computed both global and local ASA markers and we compared them with SA indexes. Over stationary HP series we found that: i) ASA provides a general method to decompose HP variance according to symbolic pattern classes; ii) ASA is useful to describe cardiac control; iii) ASA indexes are complementary to SA markers; iv) ASA emphasizes the link of HP variability markers expressed in absolute units with vagal control; v) global and local ASA approaches provide similar information. SA and ASA should be utilized concomitantly for a deeper characterization of cardiac control from spontaneous HP fluctuations.

1. Introduction

Heart period (HP) fluctuates about its mean in the range of frequencies below 0.5 Hz, and the amount of these changes has been linked to the autonomic control targeting the heart [1]. Autonomic markers are computed via spectral analysis decomposing the power of stationary HP series into fractions that can be attributed to specific frequency bands, mainly the low frequency (LF, from 0.04 to 0.15 Hz) and high frequency (HF, from 0.15 to 0.5 Hz) bands. The HF power of HP oscillations, taken as a marker of respiratory sinus arrhythmia [2], is a widely recognized marker of vagal modulation [3]. As a matter of fact, this portion of the total variability has been abolished by cholinergic blockade induced by high-dose administration of atropine [3–7], even though sympathetic circuits can modulate respiratory sinus arrhythmia by modifying the inhibitory action of sympathetic control on the vagal drive [8]. Interpretation of markers related to HP fluctuations in the LF band is more

* Corresponding author. Università degli Studi di Milano Dipartimento di Scienze Biomediche per la Salute IRCCS Policlinico San Donato Laboratorio di Modellistica di Sistemi Complessi, Via R. Morandi 30 20097, San Donato Milanese, Milano, Italy.
E-mail address: alberto.porta@unimi.it (A. Porta).

https://doi.org/10.1016/j.compbiomed.2026.111473
Received 21 November 2025; Received in revised form 24 December 2025; Accepted 10 January 2026
Available online 16 January 2026

controversial given that muscarinic blockade affects the LF power of HP variability [3–7], the cardiac arm of baroreflex modulates autonomic outflow in LF band [9,10] and burst rate of sympathetic outflow oscillates according to LF rhythms [11–13]. However, it has been proposed that suitable normalizations can reduce the impact of the variance on the LF power of HP variability indexes, thus emphasizing the contribution of sympathetic control [14,15].

Symbolic analysis (SA) is a model-free tool commonly utilized for the characterization of stationary HP sequences due to its ability to discard irrelevant details, while enhancing specific features of the dynamics [16]. SA is grounded on: i) a coarse graining approach transforming the original time course into a symbolic series; ii) a procedure concatenating several symbols into patterns; iii) a strategy clustering patterns with similar meaning into a small number of classes; iv) the evaluation of the rate of the pattern families. SA is commonly used to describe HP variability because of its efficiency in extracting and classifying dynamical features [17–41]. However, SA is focused on the computation of the rates of occurrence of symbolic patterns, or pattern families, thus producing normalized markers ranging from 0 to 1, or eventually expressed as percentages, while disregarding the contribution of a pattern class to the total variability [42,43]. This lack prevents the exploitation of the pattern classification strategy adopted by the SA to decompose the variance of the series and derive HP variability indexes that are expressed in square units of the measured variable.

The aim of this study is to propose amplitude SA (ASA) as a tool able to introduce the amplitude of changes between adjacent samples of a pattern in SA and to assess the contribution of symbolic pattern classes to the HP variance. The ability of ASA is made evident on three classical protocols designed to evaluate the impact of autonomic nervous system (ANS) on cardiovascular control complexity in physiological and pathological conditions, namely during a pharmacological challenge (PC) in healthy individuals [44,45], a graded head-up tilt (GHUT) in healthy subjects [46] and a postural challenge in Parkinson disease (PD) patients [47]. Preliminary results were presented to Computing in Cardiology 2025 [48].

2. Analyzing a time series via symbolic computation

2.1. SA

We followed the SA approach described in Refs. [22,34]. Briefly, the series $y = \{y_n, n = 1,\ldots,N\}$, where n is the progressive beat counter and N is the series length, was coarse-grained by subdividing the min-max range into ξ bins of equal amplitude. Each original value y_n was substituted with an integer value y_n^{ξ} ranging from 0 to $\xi-1$ and labelling the bin y_n belonged to, thus transforming y into a symbolic series $y^{\xi} = \{y_n^{\xi}, n = 1, \ldots, N\}$. The delay embedding procedure was followed to create the m-dimensional pattern $\boldsymbol{y}_{m,j}^{\xi} = \left[\, y_j^{\xi} \quad y_{j-1}^{\xi} \quad \cdots \quad y_{j-m+1}^{\xi} \,\right]$. According to previous recommendations, N was set to 256 to focus short-term cardiac control mechanisms [1], while ξ and m were set to 6 and 3 respectively to ensure that the probability of finding a symbolic pattern can be reliably approximated with its relative frequency [22]. To reduce the number of possible patterns (*i.e.*, ξ^m) into a small number of meaningful categories, each pattern $\boldsymbol{y}_{m=3,j}^{\xi=6}$ was classified into four classes according to the number and sign of variations between adjacent components: i) no variation (0V) featuring three equal symbols; ii) one variation (1V) presenting two consecutive equal symbols, while the third one was different; iii) two like variations (2LV) featuring two non-zero variations of the same sign between adjacent symbols; iv) two unlike variations (2UV) presenting two non-zero variations of opposite sign between adjacent symbols. This strategy, reducing the redundancy of patterns generated by symbolization procedure, categorizes symbolic patterns according to variability of symbols from the most stable symbolic pattern (*i.e.*, 0V) to the most variable symbolic pattern (*i.e.*, 2UV) with 1V less stable than 0V and 2LV less variable than 2UV [22,43]. Since any pattern $\boldsymbol{y}_{m=3,j}^{\xi=6}$, with $j = 1, \ldots, N-m+1$, fell into one, and only one, category, the sum of the number of 0V, 1V, 2LV and 2UV patterns was $N-m+1$ with $m = 3$. The rate of occurrence of a pattern class was estimated as the ratio of the number of patterns to $N-m+1$ multiplied by 100 with $m = 3$. These indexes were labelled as 0V%, 1V%, 2LV% and 2UV%, and expressed as percentage (%). Because of the definition 0V% + 1V% + 2LV% + 2UV% = 100%.

2.2. Global and local ASA

The ASA approach introduced in SA the concept of the amplitude of the variations between adjacent samples forming $\boldsymbol{y}_{m=3,j}^{\xi=6}$. The global approach utilized the global mean of y for the assessment of deviation of each original values, while the local approach computed the local mean over each pattern and variations were computed with respect to the local mean.

The global sum (S_g) of square deviations is defined as

$$S_g = \sum_{n=1}^{N-m+1} \sum_{i=0}^{m-1} (y_{n+i} - \mu)^2, \tag{1}$$

with $m = 3$, where

$$\mu = \frac{1}{N} \sum_{n=1}^{N} y_n, \tag{2}$$

is the global mean. The S_g can be factorized into four terms representing the sum of square deviations from μ computed over all the patterns belonging to 0V, 1V, 2LV and 2UV pattern families respectively. These portions of S_g are labelled $S_{g,0V}$, $S_{g,1V}$, $S_{g,2LV}$, and $S_{g,2UV}$, respectively with

$$S_g = S_{g,0V} + S_{g,1V} + S_{g,2LV} + S_{g,2UV}. \tag{3}$$

The local sum (S_l) of square deviations is defined as

$$S_l = \sum_{n=1}^{N-m+1} \sum_{i=0}^{m-1} (y_{n+i} - \mu_n)^2, \tag{4}$$

with $m = 3$, where

$$\mu_n = \frac{1}{m} \sum_{i=0}^{m-1} y_{n+i}. \tag{5}$$

is the local mean. Like S_g, even S_l can be factorized into four terms representing the sum of square deviations from μ_n computed over the patterns belonging to 0V, 1V, 2LV and 2UV pattern families respectively. These portions of S_l are labelled $S_{l,0V}$, $S_{l,1V}$, $S_{l,2LV}$, and $S_{l,2UV}$, respectively with

$$S_l = S_{l,0V} + S_{l,1V} + S_{l,2LV} + S_{l,2UV}. \tag{6}$$

Defined the variance σ^2 of y as

$$\sigma^2 = \frac{1}{N-1} \sum_{n=1}^{N} (y_n - \mu)^2, \tag{7}$$

global ASA markers are computed as the ratio of $S_{g,0V}$, $S_{g,1V}$, $S_{g,2LV}$, and $S_{g,2UV}$ to S_g multiplied by σ^2. Analogously, the local ASA markers are calculated as the ratio of $S_{l,0V}$, $S_{l,1V}$, $S_{l,2LV}$, and $S_{l,2UV}$ to S_l multiplied by σ^2. The global ASA markers are labelled $a0V_g$, $a1V_g$, $a2LV_g$, and $a2UV_g$, while local ASA markers are labelled $a0V_l$, $a1V_l$, $a2LV_l$, and $a2UV_l$ respectively. Global and local ASA indexes are expressed in ms^2. Because of the definition $a0V_g + a1V_g + a2LV_g + a2UV_g = \sigma^2$ and $a0V_l + a1V_l + a2LV_l + a2UV_l = \sigma^2$.

3. Experimental protocol and data analysis

3.1. Influence of drugs affecting the ANS: the PC protocol in healthy subjects

This protocol was originally designed to investigate the impact of the autonomic control on HP variability through the administration of drugs able to selectively block the vagal and/or sympathetic branches of the ANS [44]. A detailed description of the PC protocol in healthy subjects can be found in Ref. [44]. The protocol adhered to the principles of the Declaration of Helsinki for medical research involving human subjects. The human research and ethical review board of the Hospices Civils de Lyon approved the protocol. All the subjects gave their written informed consent. We studied 9 healthy volunteers (age: 25–46 yrs, 9 males) recruited within the community of the physicians of the hospital and familiar with the study setting. Physical examination and electrocardiography confirmed the healthy status of the subjects. None of the subjects were under pharmacological treatment. All had no history of hypertension, and their normal resting brachial arterial pressure was verified by a sphygmomanometer before starting the experimental session. The subjects were instructed to avoid tobacco, alcohol and caffeine for 12 h and strenuous exercise for 24 h before each experiment. During the experiment the subjects breathed spontaneously, and they refrained from talking. Electrocardiogram (ECG) was recorded during each experimental session. Signals were sampled at 500 Hz. Experiments were performed on 3 different days at approximately 2-week intervals. One volunteer took part only in the experiments carried out during the first day. Each experiment started in the morning (from 08:00 to 09:00). Subjects remained at rest in supine position before starting a baseline (B) recording lasting 15–20 min. The B period was followed by 15–20 min of recording after drug administration. Recordings were obtained: i) on day 1 after the intravenous administration of 40 $\mu g \cdot kg^{-1}$ atropine sulfate (AT) to induce vagal blockade through the inhibition of muscarinic acetylcholine receptors; ii) on day 2 after the intravenous administration of 200 $\mu g \cdot kg^{-1}$propranolol (PR) to induce β-adrenergic blockade via the inhibition of β1 cardiac and β2 vascular peripheral adrenergic receptors; iii) on day 1 PR was administered at the end of the AT session (the dose of AT was reinforced by 10 $\mu g \cdot kg^{-1}$) to combine the effect of AT and PR (AT + PR) and obtain the blockade of cardiac parasympathetic and sympathetic branches of the ANS; iv) on day 3 recordings were obtained 120 min after oral ingestion of 6 $\mu g \cdot kg^{-1}$ clonidine hydrochloride (CL) to centrally block the sympathetic outflow to heart and vasculature and to centrally increase the cardiac parasympathetic activity [45].

3.2. Effects of an orthostatic stimulus of controlled intensity: GHUT protocol in healthy subjects

This protocol was originally designed to monitor the progressive impact of autonomic control on HP variability with the magnitude of the postural challenge monitored via the inclination of the tilt table [46]. A detailed description of the GHUT protocol can be found in Ref. [46]. The study was in keeping with the principles of the Declaration of Helsinki for medical research involving human subjects. The human research and ethical review boards of the "L. Sacco" Hospital and of the Department of Biomedical and Clinical Sciences approved the protocol. Written informed consent was obtained from all subjects. We studied 19 healthy volunteers (age: 21–48 yrs, median = 30 yrs; 8 males). All the subjects had no history and no clinical evidence of any disease. They were free from any medications. They refrained from consuming any caffeine or alcohol-containing beverages during the 24 h before the recordings as well as from strenuous physical exercise. All the experiments were performed in the morning. The subjects were on the tilt table supported by two belts at the level of thigh and waist respectively and with both feet touching the footrest of the tilt table. ECG (lead II) was recorded. Sampling frequency was 300 Hz. A period of 5 min for acclimatization with laboratory conditions and instrumentation was allowed while resting in horizonal position at B. After this period, recordings were performed in the same order: 1) at B for 7 min; 2) during head-up tilt regardless of table inclination (T) for 10 min; 3) during recovery for 8 min. The inclination of the tilt table, expressed in degrees, was randomly chosen within the set {15,30,45,60,75,90} (T15, T30, T45, T60, T75, T90). Each subject experienced all the tilt table inclinations and completed the entire sequence without experiencing any signs of pre-syncope. To allow the stabilization of the physiological variables analyses were performed after about 2 min from the onset of each experimental condition. During the entire protocol the subjects breathed spontaneously but they were not allowed to talk.

3.3. Impact of ANS impairment: the PD protocol

This protocol was originally designed to assess autonomic control in PD patients from HP variability as probed via a postural challenge and compared to healthy control (HC) subjects [47]. A detailed description of the PD protocol can be found in Ref. [47]. The study adhered to the principles of the Declaration of Helsinki for medical research involving human subjects. The human research and ethical review boards of the Bolognini Hospital of Seriate, Bergamo, Italy approved the protocol. All the subjects gave their written informed consent. We studied 12 PD patients without orthostatic hypotension or symptoms of orthostatic intolerance (age: 55–79 yrs, median = 65 yrs, 8 males) and 12 HC subjects matched by age and gender with the PD group (age: 58–72 yrs, median = 67 yrs, 7 males). HC individuals were recruited from hospital and university staff, and among PD patients' relatives featuring no significant past medical history of cardiovascular, neurological, or respiratory diseases. The PD patents (2–4 Hoehn-Yhar scale) were at the best of their habitual pharmacological treatment. We recorded ECG (lead II). Signals were sampled at 300 Hz. Signals were recorded with the subject lying on the tilt table, gently fastened by two belts at the level of the thigh and waist, with both feet touching the footrest of the tilt table. Recordings of 10 min were obtained at B and during T75. During the protocol, the subjects were breathing spontaneously but were not allowed to talk.

3.4. Beat-to-beat HP variability series

After detecting the R-wave peaks on the ECG using a traditional method based on a threshold on its first derivative, the time distance between two consecutive R-wave peaks was labelled as the nth HP. The jitters in locating the R-wave peak were minimized using parabolic interpolation. Detections of the R-wave peaks were visually checked: missed R-waves were manually inserted and erroneous identification were deleted and reinserted if necessary. In these cases all the HPs affected by the correction were recalculated. ECG recordings were free of complex arrhythmic episodes. The effect of isolated arrhythmic beats on the HP variability series was mitigated through linear interpolation using the two most adjacent HP values delimited by sinus beats. The limit of 5 % of corrections was never reached. SA and ASA markers were computed over HP series. Sequences were randomly selected within the experimental sessions. All the sequences underwent linear detrending to mitigate the impact on nonstationarities. The stability of the mean and variance was checked to ensure the fulfillment of weak stationarity [48].

3.5. Statistical analysis

The Shapiro-Wilk test was carried out to verify the normality of the distribution and Brown-Forsythe test to check homoscedasticity. In the PC protocol one-way analysis of variance, or Kruskal-Wallis one-way analysis of variance on ranks when appropriate, was applied (Dunn's test for multiple comparisons versus B) to check the impact of the autonomic blockades compared to B. In the GHUT protocol linear regression analysis of SA and ASA markers on tilt table angle was carried out. Linear regression analysis was carried out after pooling together all subjects

and at individual level. Pearson product moment correlation r and type-I error probability p was reported when the linear correlation analysis was carried out after pooling together all the subjects, while the percentage of subjects exhibiting a significant association with tilt table angles was given when the analysis was performed at individual level. In the PD protocol two-way repeated measures analysis of variance was performed (one factor repetition, Holm-Sidak method for multiple comparisons) to assess the significance of changes of SA or ASA indexes induced by the orthostatic challenge within the same population (*i.e.*, HC or PD group) and the difference between groups within the same experimental condition (*i.e.*, B or T75). If normality and equal variance tests for the application of Holm-Sidak test were not passed, the corresponding non-parametric tests (*i.e.*, Mann-Whitey rank sum and Wilcoxon signed-rank tests) were applied. In this case the level of significance was divided by the number of comparisons (*i.e.*, 4) to account for the multiple comparison issue. The degree of linear association of ASA indexes with SA ones computed over the same pattern family was evaluated via linear regression analysis in each experimental protocol. Experimental conditions were pooled together before performing linear correlation analysis. All the statistical analyses were performed with a commercial statistical software (Sigmaplot v.14.0, Systat Software, San Jose, CA, USA). The level of statistical significance of all the tests was set to 0.05. A p smaller than the level of significance was always taken as significant.

4. Results

4.1. Results of SA and ASA in PC, GHUT and PD protocols

The vertical box-and-whisker plots of Fig. 1 show markers of traditional SA, namely 0V% (Fig. 1a), 1V% (Fig. 1b), 2LV% (Fig. 1c) and 2UV% (Fig. 1d), as a function of the experimental condition (*i.e.*, B, AT, PR, AT + PR, and CL) in the PC protocol. After AT 0V% increased significantly compared to B, while 1V%, 2LV% and 2UV% decreased. After CL 2UV% rose significantly compared to B, while 0V%, and 1V% declined. After AT + PR the sole significant variation with respect to B was the drop of 2LV%.

Fig. 2 has the same structure as Fig. 1 but it shows ASA markers computed according to a global approach, namely $a0V_g$ (Fig. 2a), $a1V_g$ (Fig. 2c), $a2LV_g$ (Fig. 2e) and $a2UV_g$ (Fig. 2g), and to a local approach, namely $a0V_l$ (Fig. 2b), $a1V_l$ (Fig. 2d), $a2LV_l$ (Fig. 2f) and $a2UV_l$ (Fig. 2h), in the PC protocol. AT and AT + PR induced a significant decrease of all the ASA indexes compared to B. $a0V_g$ and $a0V_l$, decreased after CL, while $a2UV_g$ increased. PR did not affect any ASA markers.

The scatter plots of Fig. 3 show the result of the linear correlation analysis of traditional SA markers, namely 0V% (Fig. 3a), 1V% (Fig. 3b), 2LV% (Fig. 3c) and 2UV% (Fig. 3d), on tilt table angle in the GHUT protocol. Values of r and p were computed over all subjects. 0V% increased gradually with the magnitude of the orthostatic challenge with $r = 0.558$ and $p = 2.99 \times 10^{-12}$. Conversely, 2LV% and 2UV% decreased progressively with tilt table inclination with $r = -0.401$ and $p = 1.70 \times 10^{-6}$, and $r = -0.549$ and $p = 7.51 \times 10^{-12}$ respectively. 1V% remained stable during the GHUT protocol with $r = 0.081$ and $p = 3.52 \times 10^{-1}$. Linear regression analysis was carried out individually as well. The percentage of subjects exhibiting a significant individual correlation were 74 %, 11 %, 37 % and 63 % in the case of 0V%, 1V%, 2LV% and 2UV% respectively.

Fig. 4 has the same structure as Fig. 3 but it shows the result of linear correlation analysis of ASA markers computed according to a global approach, namely $a0V_g$ (Fig. 4a), $a1V_g$ (Fig. 4c), $a2LV_g$ (Fig. 4e) and $a2UV_g$ (Fig. 4g), and to a local approach, namely $a0V_l$ (Fig. 4b), $a1V_l$ (Fig. 4d), $a2LV_l$ (Fig. 4f) and $a2UV_l$ (Fig. 4h), on tilt table angle in the GHUT protocol. Values of r and p were computed over all subjects. $a0V_g$ and $a0V_l$ increased gradually with the magnitude of the postural challenge with $r = 0.202$ and $p = 1.97 \times 10^{-2}$, and $r = 0.247$ and $p = 4.22 \times 10^{-3}$ respectively. Conversely, $a1V_g$, $a1V_l$, $a2LV_g$, $a2LV_l$, $a2UV_g$ and $a2UV_l$ decreased progressively with $r = -0.306$ and $p = 3.35 \times 10^{-4}$, $r = -0.235$ and $p = 6.51 \times 10^{-3}$, $r = -0.421$ and $p = 4.42 \times 10^{-7}$, $r = -0.281$ and $p = 1.03 \times 10^{-3}$, $r = -0.465$ and $p = 1.67 \times 10^{-8}$, and $r = -0.432$ and $p = 2.01 \times 10^{-7}$, respectively. Linear regression analysis was carried out individually as well. The percentage of subjects exhibiting a significant individual correlation were 16 %, 21 %, 58 % and 68 % in the case of $a0V_g$, $a1V_g$, $a2LV_g$ and $a2UV_g$ respectively and 32 %, 21 %, 42 % and 74 % in the case of $a0V_l$, $a1V_l$, $a2LV_l$ and $a2UV_l$ respectively.

The vertical grouped box-and-whiskers plots of Fig. 5 show traditional SA markers, namely 0V% (Fig. 5a), 1V% (Fig. 5b), 2LV% (Fig. 5c) and 2UV% (Fig. 5d), as a function of the experimental condition (*i.e.*, B and T75) in the PD protocol. Markers were computed in HC subjects (white bars) and PD patients (gray bars). Regardless of the experimental condition, 1V% significantly decreased in the PD group compared to

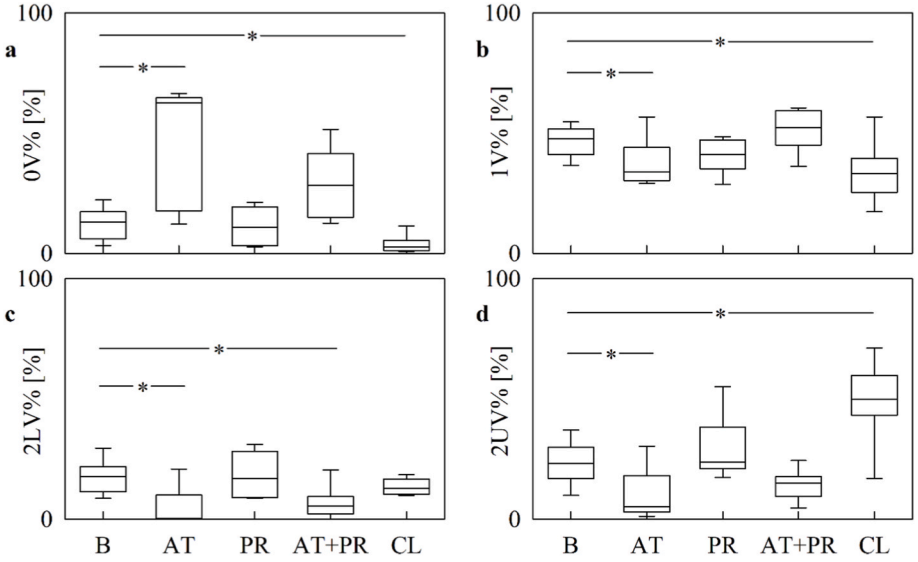

Fig. 1. The vertical box-and-whiskers plots show the 5th, 25th, 50th, 75th and 95th percentiles of traditional SA markers, namely 0V% (a), 1V% (b), 2LV% (c) and 2UV% (d) computed in the PC protocol. Indexes are reported as a function of the experimental condition (*i.e.*, B, AT, PR, AT + PR and CL). The height of the box represents the interquartile range with the median indicated as a horizontal line, while the whiskers correspond to the 5th and 95th percentiles. The symbol * indicates $p < 0.05$ vs B.

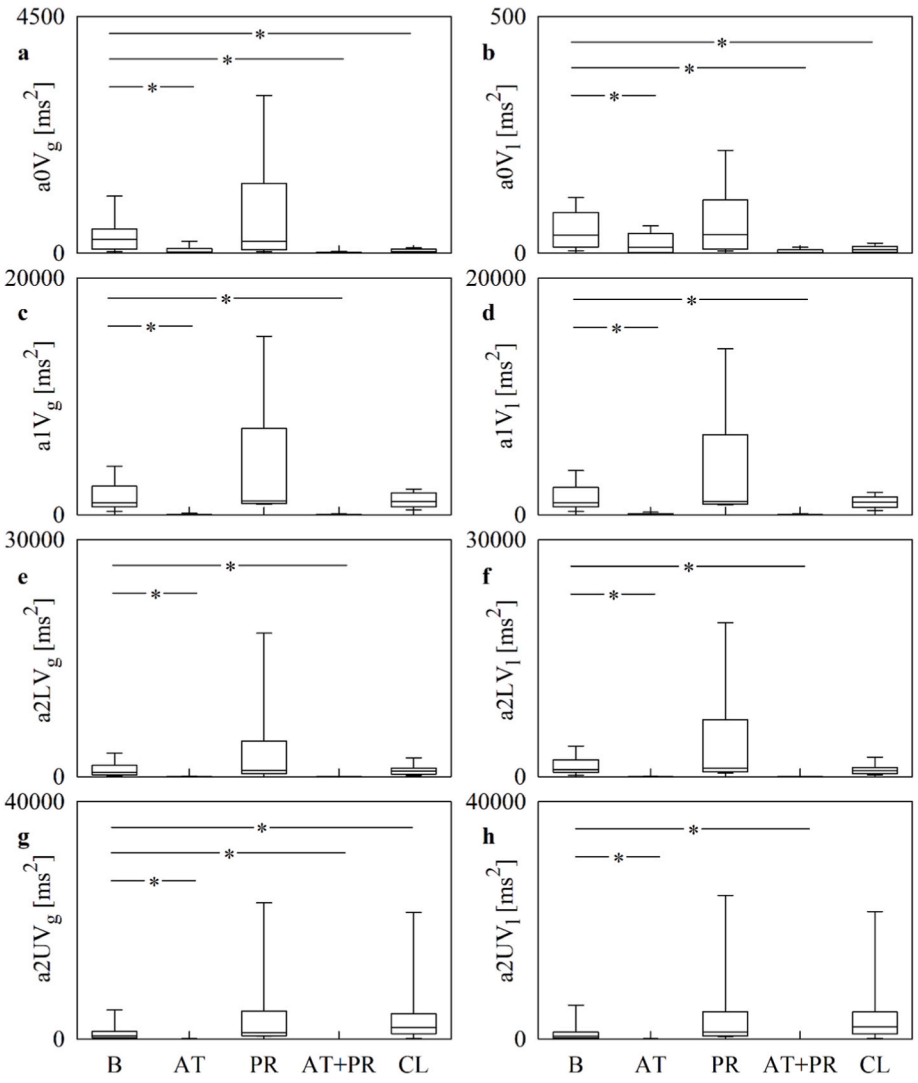

Fig. 2. The vertical box-and-whiskers plots show the 5th, 25th, 50th, 75th and 95th percentiles of ASA markers derived from global approach, namely $a0V_g$ (a), $a1V_g$ (c), $a2LV_g$ (e) and $a2UV_g$ (g), and from local approach, namely $a0V_l$ (b), $a1V_l$ (d), $a2LV_l$ (f) and $a2UV_l$ (h), computed in the PC protocol. Indexes are reported as a function of the experimental condition (*i.e.*, B, AT, PR, AT + PR and CL). The height of the box represents the interquartile range with the median indicated as a horizontal line, while the whiskers correspond to the 5th and 95th percentiles. The symbol * indicates $p < 0.05$ vs B.

HCs, while 1V% did not vary with the postural challenge in either the group. 2UV% increased in the PD group compared to HCs only during T75, while the impact of the orthostatic stimulus was visible exclusively in the HC group and took the form of the decrease of 2UV% during T75 compared to B. 0V% and 2LV% did not change across either groups or experimental conditions.

Fig. 6 has the same structure as Fig. 5 but it shows ASA markers computed according to a global approach, namely $a0V_g$ (Fig. 6a), $a1V_g$ (Fig. 6c), $a2LV_g$ (Fig. 6e) and $a2UV_g$ (Fig. 6g), and to a local approach, namely $a0V_l$ (Fig. 6b), $a1V_l$ (Fig. 6d), $a2LV_l$ (Fig. 6f) and $a2UV_l$ (Fig. 6h), in the PD protocol. Solely $a0V_g$ varied during the protocol: more specifically, $a0V_g$ decreased significantly in PD patients compared to HCs during T75. This tendency was evident regardless of the ASA marker, thus suggesting an impaired response to postural challenge in PD patients compared to HCs. No significant changes were observed across experimental conditions.

4.2. Results of correlation analysis between SA and ASA markers

Table 1 shows the results of correlation analysis between SA and ASA markers derived from the same pattern family in the PC protocol. Analyses were carried out over global and local ASA indexes. Data were pooled together regardless of the experimental session. SA and ASA markers computed over more stable patterns (*i.e.*, 0V and 1V) were uncorrelated, while those calculated over more variable patterns (*i.e.*, 2LV and 2UV) were significantly and positively associated. Results held regardless of the approach (*i.e.*, local or global).

Table 2 has the same structure as Table 1 but it shows the results of correlation analysis in the GHUT protocol. Data were pooled together regardless of the tilt table inclination. Results were reported distinctly over global and local ASA indexes. 1V% and a1V indexes were uncorrelated. Conversely, SA and ASA markers computed over patterns featuring invariable symbols (*i.e.*, 0V) or highly variable patterns (*i.e.*, 2LV and 2UV) were significantly and positively associated. Results held regardless of the approach (*i.e.*, local or global).

Table 3 shows the results of correlation analysis between SA and ASA markers derived from the same pattern family in the PD protocol as a function of the population. Analyses were carried out over global and local ASA markers. Within the HC and PD groups data were pooled together regardless of the experimental condition. Regardless of global or local approach to the assessment of ASA indexes, we found a significant and positive association when considering 2LV and 2UV patterns.

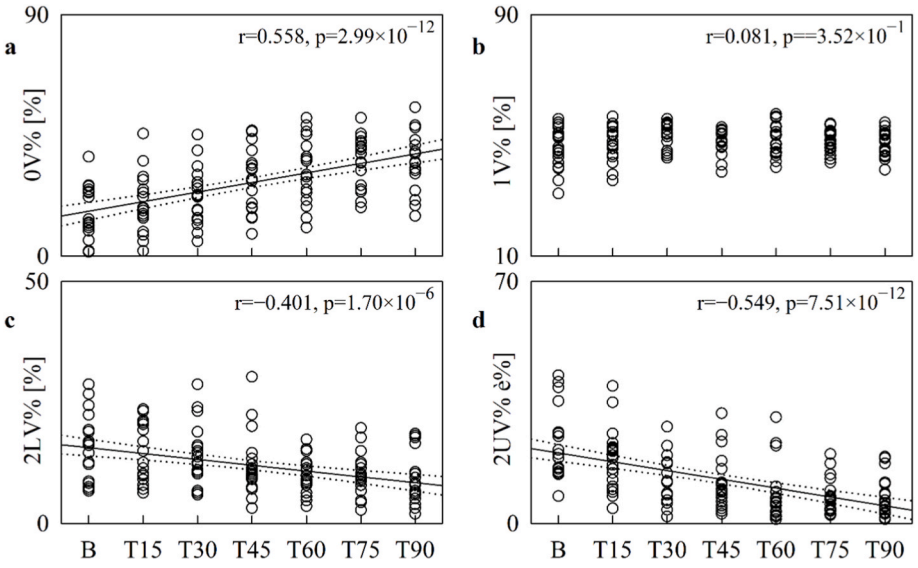

Fig. 3. The scatter plots show the linear correlation analysis of traditional SA markers, namely 0V% (a), 1V% (b), 2LV% (c) and 2UV% (d) on tilt table inclination computed in the GHUT protocol. Each open circle represents the value of the marker computed over a subject in each experimental condition (*i.e.*, B, T15, T30, T45, T60, T75, and T90). The linear regression (solid line) and its 95 percent confidence interval (dotted lines) are plotted when a significant association between the marker and tilt table inclination is found.

Conversely, SA and ASA indexes derived from pattern families with more limited symbol variability exhibited insignificant, or more limited, association and results could be different when considering global and local indexes.

5. Discussion

The main findings of this study over stationary HP sequences can be summarized as follows: i) ASA is a SA-based method providing a way to decompose the HP variance; ii) SA detects changes of the cardiac control induced by autonomic challenges in healthy and pathological individuals; iii) ASA emphasizes the link of HP variability markers expressed in absolute units with the vagal control; iv) global and local ASA approaches provide similar information; v) ASA supplements the information provided by SA.

5.1. ASA: a SA-based method providing a way to decompose the variance of a time series

Symbolic computation operates over stationary series and makes use of coarse graining techniques to transform the original HP values into symbols and grouping strategies for building symbolic patterns [16,42,43]. Symbolization strategies are commonly based on the amplitude of dynamics [17,18,21,22,25–28,34,39,41], variations between consecutive values [17–19,20,23,24,28–30,32,35,37,38,40], or ranking of components of the pattern [31,33,36]. Definition of symbolic features allows the efficient estimation of the likelihood of finding a specific symbolic pattern in the HP variability series via its relative frequency. The evaluation of the probability distribution of symbolic patterns ensures the evaluation of the complexity of HP variability via the estimation of the Shannon entropy or the conditional entropy computed as the variation of Shannon entropy [22,26]. Since the symbolization strategies based on amplitude of the dynamics utilized a fixed amount of symbols regardless the values assumed by the minimum and the maximum of the series [17,18,21,22,25–28,34,39,41], those grounded on variations between consecutive values disregard the amplitude of the changes [17–19,20,23,24,28–30,32,35,37,38,40], and those on ranking of components of the pattern accounts solely for the order of the values [31,33,36], SA does not account explicitly for the magnitude of changes between consecutive samples forming the patterns. As a matter of fact, symbolic features belonging to the same class might differ dramatically in the amount of variability across original samples. Consequently, SA disregards the important information related to the amplitude of variations. Fig. 7 exemplifies this concept according to a symbolization strategy based on amplitude of HP dynamics: symbolic patterns (Fig. 7b, d) belonging to the same class, namely 2UV in this representative example, refer to original patterns with dramatically different variability across HP values (Fig. 7a,c). Normalization provided by SA might be limitative in HP variability analysis because the amplitude of changes between consecutive HPs contains relevant information about ANS functioning, especially about vagal control that plays an important role in regulating fast HP components [3–7]. ASA introduces the amplitude of changes between adjacent components of the patterns in SA. ASA is based on: i) a pattern classification and redundancy reduction strategy defined according to a traditional SA approach; ii) the computation of the overall sum S of square deviations of any component of the original patterns from the mean; iii) the computation of the fractional contribution of any symbolic class to the S; iv) the rescaling of this fraction to the variance of HP variability series to assess the portion of the HP variance explained by the symbolic class. Remarkably, ASA features two important properties: 1) the sum of the indexes over all the symbolic classes is the variance of the HP variability series, thus providing a way to decompose the HP power according to pattern classification strategy defined by SA; 2) the approach is independent of the symbolization approach, definition of symbolic patterns and strategy followed to group patterns into a small number of classes. In the present study we utilized a symbolic approach based on a uniform quantization procedure over $\xi = 6$ bins, on the formation of patterns of length $m = 3$ using the technique of delayed embedding and on a redundancy reduction strategy grouping patterns into four categories defined according to the number and sign of variations between adjacent symbols [22,34]. Nevertheless, the proposed ASA method can be applied with symbolization procedures based on amplitude of the dynamics, the sign of variation between original values, or ranking statistics [17–41], with pattern formation strategies alternative to the delay embedding [49], and with methods clustering patterns into families based on entropy [19].

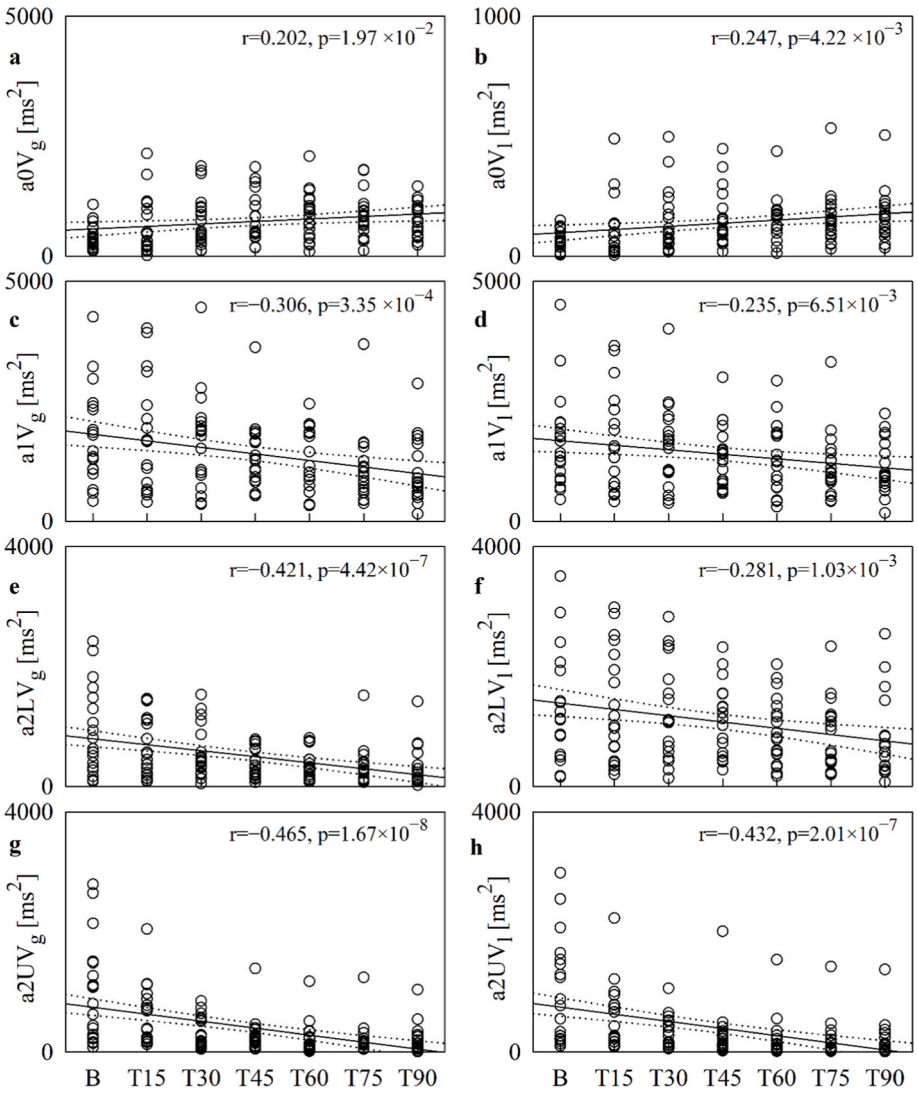

Fig. 4. The scatter plots show the linear correlation analysis of ASA markers derived from global approach, namely $a0V_g$ (a), $a1V_g$ (c), $a2LV_g$ (e) and $a2UV_g$ (g), and from local approach, namely $a0V_l$ (b), $a1V_l$ (d), $a2LV_l$ (f) and $a2UV_l$ (h), on tilt table inclination in the GHUT protocol. Each open circle represents the value of the marker computed over a subject in each experimental condition (*i.e.*, B, T15, T30, T45, T60, T75, and T90). The linear regression (solid line) and its 95 percent confidence interval (dotted lines) are plotted when a significant association between the marker and tilt table inclination is found.

5.2. SA describes modifications of the cardiac control induced by autonomic challenges in healthy and pathological individuals

SA detects the reduced vagal control induced by GHUT [11,15], the pharmacological peripheral vagal blockade induced by the administration of a high dose of AT [3–7], and the pharmacological central vagal modulation enhancement induced by the administration of CL [45]. Vagal control inhibition was stressed by the progressive decrease of likelihood of finding highly variable patterns, such as 2LV and 2UV, with the magnitude of the orthostatic challenge during GHUT and by the dramatic decline of the presence of 2LV and 2UV patterns after AT. Conversely, vagal control activation was highlighted by the increase of 2UV% after CL. The rise of 0V% suggests the gradual increase of the sympathetic modulation proportional to tilt table inclination during GHUT [11–13] and the shift of the sympatho-vagal balance toward a prevalence of the sympathetic control during AT [7]. The decrease of 0V % and 1V% during CL was an indication of the direct central sympathetic inhibition [46] and the inhibitory action of vagal circuits on the sympathetic control [8].

Signs of dysautonomia are commonly observed in PD patients [50–52]. The cardiac control impairment was suggested by the reduction of total power of HP series [53–55], the decline of fraction of the HP variability in the LF band [53,54,56] as a likely consequence of a limited HP response to arterial pressure changes [47,54,55,57], the reduction of the tonic sympathetic activity [47,58], the inadequate sensitivity of the cardiac arm of the baroreflex [47,55,57,58], the blunted drop of the HF power of HP variability and cardiac baroreflex sensitivity during postural challenge [47,55], and the inability of arterial pressure modifications to drive HP changes [59,60]. The reduction of HP variability was made evident by the decrease of 1V% both at B and during T75, while the impairment of the cardiac control response to stressors was highlighted by the missed decrease of 2UV% during T75 in the PD group that made the likelihood of finding 2UV patterns during T75 higher in PD patients than in HCs.

5.3. ASA emphasizes the link of markers of HP variability expressed in absolute units with the vagal control

ASA approaches suggested that HP variability markers expressed in absolute units (*i.e., ms*^{2}*) are mainly under vagal control. Indeed, even in presence of a SA marker sensitive to sympathetic control such as 0V% the portion of HP variability explained by this pattern, as estimated via a0V, was*

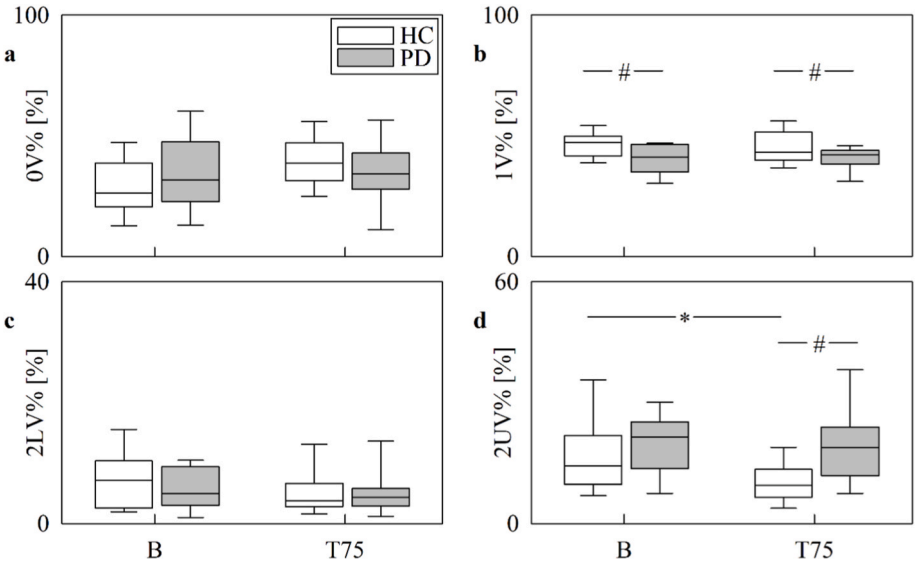

Fig. 5. The vertical grouped box-and-whiskers plots show the 5th, 25th, 50th, 75th and 95th percentiles of traditional SA markers, namely 0V% (a), 1V% (b), 2LV% (c) and 2UV% (d) computed in HC subjects (white box) and PD patients (gray box). Indexes are reported as a function of the experimental condition (*i.e.*, B and T75). The height of the box represents the interquartile range with the median indicated as a horizontal line, while the whiskers correspond to the 5th and 95th percentiles. The symbol # indicates $p < 0.05$ vs HC within the same experimental condition, while the symbol * indicates $p < 0.05$ vs T75 within the same group.

completely abolished by AT. However, some indications that a0V might be sensitive to sympathetic control are present: indeed, a0V *decreased after CL as a result of central sympathetic inhibition* [44,45], it gradually increased with the magnitude of sympathetic activation in GHUT protocol [11–13], and it was smaller in PD patients compared to HCs during T75 as a likely result of the sympathetic control impairment [51–53,56]. The link of ASA markers computed over highly variable symbolic patterns (*i.e.,* 2LV and 2UV) with vagal control was evident, especially when a2UV was considered. Indeed, a2UV decreased after AT [3–7], it increased during the central vagal enhancement induced by administration of CL [44,45], it decreased progressively with the relevance of the vagal withdrawal during GHUT [11,15], and it was not modified during T75 compared to B in PD patients while it decreased in HCs [47,55].

5.4. Global and local ASA approaches provide similar information over stationary HP variability series

Figs. 2, 4 and 6 allow the comparison between ASA markers derived from global (left panels) and local (right panels) approaches. This comparison suggests that the two techniques performed similarly. Indeed, differences across groups and experimental conditions in PC and PD protocols as well as trends in GHUT protocol were similar. This result is the likely consequence of the stationarity of our series. Indeed, the invariance of the mean and variance, tested during the phase of the selection of the HP frame for the analysis [61], made local and global mean very close. Only in the PD protocol the global approach produced indexes with a more limited dispersion compared to the local technique and this feature could have favored the detection of significant between-group changes.

5.5. ASA supplements information provided by SA

Correlation analysis between SA and ASA markers derived from the same symbolic class indicated a strongly significant positive association between the likelihood of finding patterns featuring rapidly varying symbolic dynamics and the amplitude of the changes across the original samples. Since the presence of rapidly varying patterns is linked to vagal control, this positive relationship stresses that the amplitude of changes at fast time scales is under vagal control [3–7]. The percentage of stable symbolic patterns is less importantly related to the amplitude of variations even though, when present, correlation coefficient is again positive. Since the presence of stable patterns is proportional to the magnitude of the sympathetic activation induced by GHUT, the positive relationship stresses that the increase of sympathetic control is associated with an augmentation of the amplitude of HP variability at slow time scales [3,11,15].

The presence of a relationship of opposite signs between SA markers and tilt table inclination in connection with the exclusive positive association between SA and ASA markers suggests that SA and ASA indexes carry complementary information. ASA markers confirm that sympathetic control contributes to HP variability at slow time scales, while vagal regulation impacts the amplitude of fast HP variations. The complementarity of SA and ASA markers was emphasized by the missing correlation between 1V% and $a1V_g$, or $a1V_l$, even though both $a1V_g$, and $a1V_l$ are more under vagal control than sympathetic one, being abolished after AT and gradually decreasing during vagal withdrawal induced by GHUT, while the reduction of 1V% in PD group compared to HCs both at B and during T75 could be related to autonomic dysfunction in PD patients.

6. Conclusions

This study proposes the ASA method for the evaluation of the cardiac autonomic function from HP variability. ASA is grounded on a SA approach, but it complements traditional SA markers based on the computation of the rate of pattern families with the evaluation of their contribution to the overall HP variance, thus providing a way to decompose the total power of HP variability series according to the definition of symbolic pattern classes given by SA. Being based on SA, ASA requires stationarity of HP sequences. However, like SA, ASA can be easily extended to nonstationary HP series by iterating over time the present approach over partially overlapped frames. Once ASA approach is properly extended to analyze nonstationary sequences, global and local ASA indexes may show important differences. Results suggest that ASA supplements information provided by SA, thus suggesting that the rate of pattern family might be independent of the contribution of the symbolic class to the overall variability of original series. Modifications of SA and ASA markers with experimental condition and/or population stress that SA indexes are more suitable to capture modifications of sympathetic control, while the ASA markers are useful to describe vagal

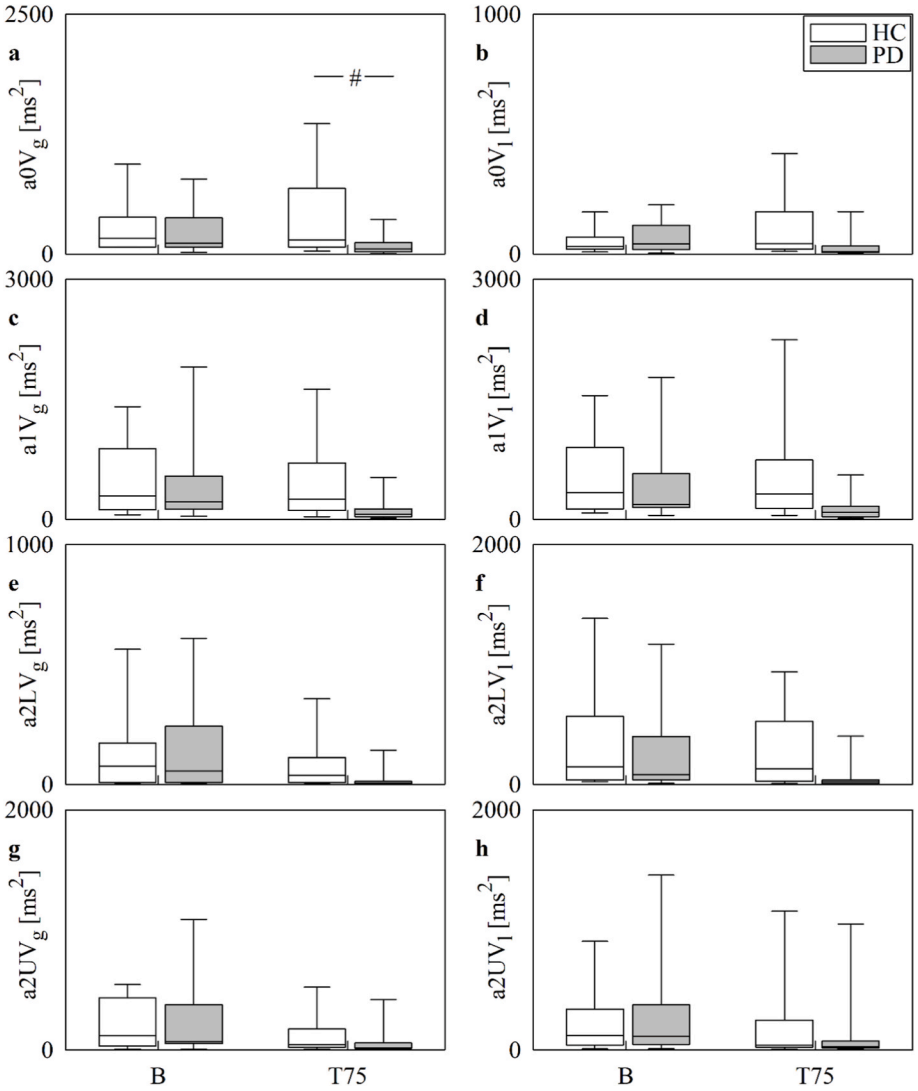

Fig. 6. The vertical grouped box-and-whiskers plots show the 5th, 25th, 50th, 75th and 95th percentiles of ASA markers derived from global approach, namely $a0V_g$ (a), $a1V_g$ (c), $a2LV_g$ (e) and $a2UV_g$ (g), and from local approach, namely $a0V_l$ (b), $a1V_l$ (d), $a2LV_l$ (f) and $a2UV_l$ (h), computed in HC subjects (white box) and in PD patients (gray box). Indexes are reported as a function of the experimental condition (*i.e.*, B and T75). The height of the box represents the interquartile range with the median indicated as a horizontal line, while the whiskers correspond to the 5th and 95th percentiles. The symbol # indicates $p < 0.05$ vs HC within the same experimental condition.

Table 1
Results of linear correlation analysis of ASA on SA markers in the PC protocol.

(x,y)	r	p
(0V%,$a0V_g$)	−0.099	4.55×10^{-1}
(1V%,$a1V_g$)	−0.194	1.40×10^{-1}
(2LV%,$a2LV_g$)	0.425	8.04×10^{-4} *
(2UV%,$a2UV_g$)	0.514	3.14×10^{-5} *
(0V%,$a0V_l$)	0.069	6.03×10^{-1}
(1V%,$a1V_l$)	−0.182	1.68×10^{-1}
(2LV%,$a2LV_l$)	0.449	3.61×10^{-4} *
(2UV%,$a2UV_l$)	0.510	3.74×10^{-5} *

0V = no variation; 1V = one variation; 2LV = two like variation; 2UV = two unlike variation; 0V% = percentage of 0V patterns; 1V% = percentage of 1V patterns; 2LV% = percentage of 2LV patterns; 2UV% = percentage of 2UV patterns; $a0V_g$ = global amplitude of 0V patterns; $a1V_g$ = global amplitude of 1V patterns; $a2LV_g$ = global amplitude of 2LV patterns; $a2UV_g$ = global amplitude of 2UV patterns; $a0V_l$ = local amplitude of 0V patterns; $a1V_l$ = local amplitude of 1V patterns; $a2LV_l$ = local amplitude of 2LV patterns; $a2UV_l$ = local amplitude of 2UV patterns; r = Pearson product moment correlation coefficient; p = type-I error probability. The symbol * indicates $p < 0.05$.

Table 2
Results of linear correlation analysis of ASA on SA markers in the GHUT protocol.

(x,y)	r	p
(0V%,$a0V_g$)	0.431	2.17×10^{-7} *
(1V%,$a1V_g$)	0.050	5.64×10^{-1}
(2LV%,$a2LV_g$)	0.705	2.73×10^{-21} *
(2UV%,$a2UV_g$)	0.752	1.83×10^{-25} *
(0V%,$a0V_l$)	0.624	9.91×10^{-16} *
(1V%,$a1V_l$)	0.043	6.23×10^{-1}
(2LV%,$a2LV_l$)	0.613	4.19×10^{-15} *
(2UV%,$a2UV_l$)	0.764	9.93×10^{-27} *

0V = no variation; 1V = one variation; 2LV = two like variation; 2UV = two unlike variation; 0V% = percentage of 0V patterns; 1V% = percentage of 1V patterns; 2LV% = percentage of 2LV patterns; 2UV% = percentage of 2UV patterns; $a0V_g$ = global amplitude of 0V patterns; $a1V_g$ = global amplitude of 1V patterns; $a2LV_g$ = global amplitude of 2LV patterns; $a2UV_g$ = global amplitude of 2UV patterns; $a0V_l$ = local amplitude of 0V patterns; $a1V_l$ = local amplitude of 1V patterns; $a2LV_l$ = local amplitude of 2LV patterns; $a2UV_l$ = local amplitude of 2UV patterns; r = Pearson product moment correlation coefficient; p = type-I error probability. The symbol * indicates $p < 0.05$.

Table 3
Results of linear correlation analysis of ASA on SA markers in the PD protocol.

(x,y)	HC		PD	
	A. *r*	*p*	*r*	*p*
(0V%,a0V_g)	0.126	5.56×10^{-1}	0.070	7.46×10^{-1}
(1V%,a1V_g)	−0.149	4.87×10^{-1}	0.227	2.85×10^{-1}
(2LV%,a2LV_g)	0.766	1.28×10^{-5} *	0.583	2.80×10^{-3} *
(2UV%,a2UV_g)	0.670	3.40×10^{-4} *	0.493	1.44×10^{-2} *
(0V%,a0V_l)	0.324	1.23×10^{-1}	0.448	1.55×10^{-2} *
(1V%,a1V_l)	−0.140	5.15×10^{-1}	0.209	3.26×10^{-1}
(2LV%,a2LV_l)	0.705	1.18×10^{-4} *	0.594	2.19×10^{-3} *
(2UV%,a2UV_l)	0.678	2.74×10^{-4} *	0.599	1.97×10^{-3} *

HC = healthy control group; PD = Parkinson disease group; 0V = no variation; 1V = one variation; 2LV = two like variation; 2UV = two unlike variation; 0V% = percentage of 0V patterns; 1V% = percentage of 1V patterns; 2LV% = percentage of 2LV patterns; 2UV% = percentage of 2UV patterns; a0V_g = global amplitude of 0V patterns; a1V_g = global amplitude of 1V patterns; a2LV_g = global amplitude of 2LV patterns; a2UV_g = global amplitude of 2UV patterns; a0V_l = local amplitude of 0V patterns; a1V_l = local amplitude of 1V patterns; a2LV_l = local amplitude of 2LV patterns; a2UV_l = local amplitude of 2UV patterns; r = Pearson product moment correlation coefficient; p = type-I error probability. The symbol * indicates $p < 0.05$.

function. We recommend the concurrent exploitation of both SA and ASA indexes to provide a more insightful description of cardiac autonomic control from spontaneous HP fluctuations. Given the efficiency of SA in classifying patterns and the limited computational costs of ASA in decomposing HP variance, the concomitant use of SA and ASA in real time monitoring is feasible. Remarkably, ASA can be applied in association with any SA method because it works regardless of the strategy adopted for symbolization, pattern construction and pattern category definition. Future studies should assess whether the application of the ASA method to different SA modalities could allow the computation of HP markers exploring different aspects of cardiac autonomic control.

CRediT authorship contribution statement

Alberto Porta: Writing – review & editing, Writing – original draft, Visualization, Validation, Supervision, Software, Resources, Project administration, Methodology, Investigation, Funding acquisition, Formal analysis, Conceptualization. **Beatrice Cairo:** Writing – review & editing, Validation, Resources, Funding acquisition, Formal analysis. **Vlasta Bari:** Writing – review & editing, Validation, Resources, Funding acquisition, Formal analysis. **Chiara Arduino:** Writing – review & editing. **Ilaria Burzo:** Writing – review & editing. **Beatrice De Maria:** Writing – review & editing. **Paolo Castiglioni:** Writing – review & editing, Validation, Data curation. **Luc Quintin:** Writing – review & editing, Validation, Data curation. **Aparecida Maria Catai:** Writing – review & editing, Validation, Data curation. **Franca Barbic:** Writing – review & editing, Validation, Data curation. **Raffaello Furlan:** Writing – review & editing, Validation, Data curation.

Ethics statement

Amplitude symbolic analysis (ASA) was tested on data acquired in three previously described protocols: a pharmacological challenge (PC) in healthy individuals [44], a graded head-up tilt (GHUT) in healthy subjects [46], and a postural challenge in Parkinson disease (PD) patients [47].

1) A detailed description of the PC protocol in healthy subjects can be found in Ref. [44]. The PC protocol adhered to the principles of the Declaration of Helsinki for medical research involving human subjects. The human research and ethical review board of the Hospices Civils de Lyon approved the protocol. All the subjects gave their written informed consent.
2) A detailed description of the GHUT protocol can be found in Ref. [46]. The GHUT protocol was in keeping with the principles of the Declaration of Helsinki for medical research involving human subjects. The human research and ethical review boards of the "L.

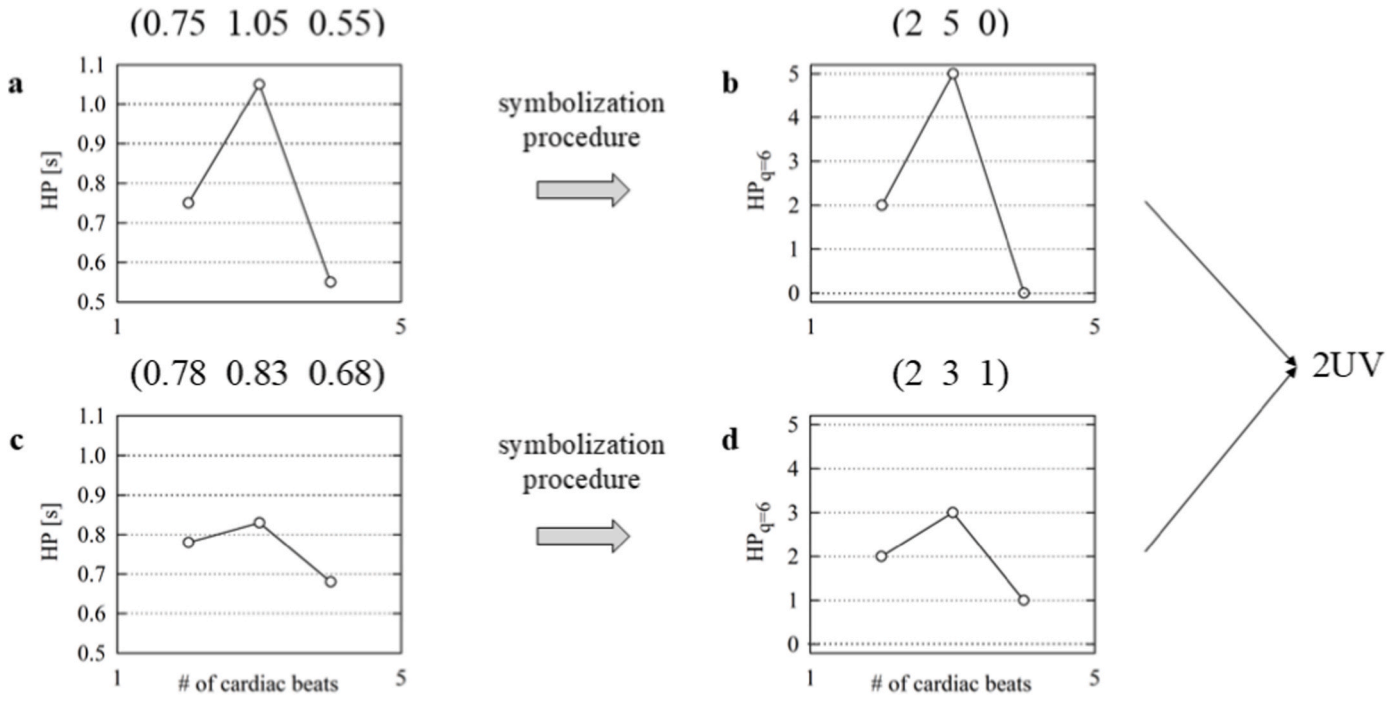

Fig. 7. The line plots show in (a) and (c) two original length-3 patterns composed by HP values dropping into different quantization bins, according to a uniform quantization procedure based on 6 bins. Both the patterns in (a) and (c) feature two opposite variations between adjacent values. Regardless of the variability of original HP values, both the patterns in (a) and (c) are transformed into symbolic 2UV patterns shown in (b) and (d) respectively. The horizontal dotted lines in (a) and (c) indicate the strips built according to the uniform 6-bin quantization procedure, while those in (b) and (d) indicate the symbols associated with each strip.

Sacco" Hospital and of the Department of Biomedical and Clinical Sciences approved the protocol. Written informed consent was obtained from all subjects.

3) A detailed description of the PD protocol can be found in Ref. [47]. The PD protocol adhered to the principles of the Declaration of Helsinki for medical research involving human subjects. The human research and ethical review boards of the Bolognini Hospital of Seriate, Bergamo, Italy approved the protocol. All the subjects gave their written informed consent.

Declaration of competing interest

The authors declare that they have no known competing financial interests or personal relationships that could have appeared to influence the work reported in this paper.

Acknowledgments

This work was partially supported by the Italian Ministry of University and Research (MUR) via the Progetto di Rilevante Interesse Nazionale (PRIN) 2022SLB5MX to Alberto Porta and by the Italian Ministry of Health via the Ricerca Corrente program to the IRCCS Policlinico San Donato.

Data availability

Datasets will be made available on reasonable request through the corresponding author.

References

[1] Task Force of the European Society of Cardiology and the North American Society of Pacing and Electrophysiology, Heart rate variability - standards of measurement, physiological interpretation, and clinical use, Circulation 93 (5) (1996) 1043–1065.

[2] J.A. Hirsch, B. Bishop, Respiratory sinus arrhythmia in humans: how breathing pattern modulates heart rate, Am. J. Physiol. 241 (4) (1981) H620–H629, https://doi.org/10.1152/ajpheart.1981.241.4.H620.

[3] B. Pomeranz, R.J. Macaulay, M.A. Caudill, I. Kutz, D. Adam, D. Gordon, K. M. Kilborn, A.C. Barger, D.C. Shannon, R.J. Cohen, H. Benson, Assessment of autonomic function in humans by heart rate spectral analysis, Am. J. Physiol. 248 (1 Pt 2) (1985) H151–H153, https://doi.org/10.1152/ajpheart.1985.248.1.H151.

[4] P.G. Katona, D. Lipson, P.J. Dauchot, Opposing central and peripheral effects of atropine on parasympathetic cardiac control, Am. J. Physiol. 232 (2) (1977) H146–H151, https://doi.org/10.1152/ajpheart.1977.232.2.H146.

[5] M. Raczkowska, D.L. Eckberg, T.J. Ebert, Muscarinic cholinergic receptors modulate vagal cardiac responses in man J. Auton, Nerv. Syst. 7 (3–4) (1983) 271–278, https://doi.org/10.1016/0165-1838(83)90080-2.

[6] J.P. Saul, R.D. Berger, P. Albrecht, S.P. Stein, M.H. Chen, R.J. Cohen, Transfer function analysis of the circulation: unique insights into cardiovascular regulation, Am. J. Physiol. 261 (4 Pt 2) (1991) H1231–H1245, https://doi.org/10.1152/ajpheart.1991.261.4.H1231.

[7] N. Montano, C. Cogliati, A. Porta, M. Pagani, A. Malliani, K. Narkiewicz, F. M. Abboud, C. Birkett, V.K. Somers, Central vagotonic effects of atropine modulate spectral oscillations of sympathetic nerve activity, Circulation 98 (14) (1998) 394–1399, https://doi.org/10.1161/01.cir.98.14.1394.

[8] J.A. Taylor, C.W. Myers, J.R. Halliwill, H. Seidel, D.L. Eckberg, Sympathetic restraint of respiratory sinus arrhythmia: implications for vagal-cardiac tone assessment in humans, Am. J. Physiol. Heart Circ. Physiol. 280 (6) (2001) H2804–H2814, https://doi.org/10.1152/ajpheart.2001.280.6.H2804.

[9] D.S. Goldstein, O. Bentho, M.-Y. Park, Y. Sharabi, Low-frequency power of heart rate variability is not a measure of cardiac sympathetic tone but may be a measure of modulation of cardiac autonomic outflows by baroreflexes, Exp. Physiol. 96 (12) (2011) 1255–1261, https://doi.org/10.1113/expphysiol.2010.056259.

[10] G. Baselli, S. Cerutti, F. Badilini, L. Biancardi, A. Porta, M. Pagani, F. Lombardi, O. Rimoldi, R. Furlan, A. Malliani, Model for the assessment of heart period and arterial pressure variability interactions and respiratory influences, Med. Biol. Eng. Comput. 32 (2) (1994) 143–152, https://doi.org/10.1007/BF02518911.

[11] W.H. Cooke, J.B. Hoag, A.A. Crossman, T.A. Kuusela, K.U.O. Tahvanainen, D. L. Eckberg, Human responses to upright tilt: a window on central autonomic integration, J. Physiol. 517 (Pt 2) (1999) 617–628, https://doi.org/10.1111/j.1469-7793.1999.0617t.x.

[12] R. Furlan, A. Porta, F. Costa, J. Tank, L. Baker, R. Schiavi, D. Robertson, A. Malliani, R. Mosqueda-Garcia, Oscillatory patterns in sympathetic neural discharge and cardiovascular variables during orthostatic stimulus, Circulation 101 (8) (2000) 886–892, https://doi.org/10.1161/01.cir.101.8.886.

[13] A. Marchi, V. Bari, B. De Maria, M. Esler, E. Lambert, M. Baumert, A. Porta, Calibrated variability of muscle sympathetic nerve activity during graded head-up tilt in humans and its link with noradrenaline data and cardiovascular rhythms, Am. J. Physiol. Regul. Integr. Comp. Physiol. 310 (11) (2016) R1134–R1143, https://doi.org/10.1152/ajpregu.00541.2015.

[14] A. Malliani, M. Pagani, F. Lombardi, S. Cerutti, Cardiovascular neural regulation explored in the frequency domain, Circulation 84 (2) (1991) 482–492, https://doi.org/10.1161/01.cir.84.2.482.

[15] N. Montano, T. Gnecchi-Ruscone, A. Porta, F. Lombardi, M. Pagani, A. Malliani, Power spectrum analysis of heart rate variability to assess the changes in sympatho-vagal balance during graded orthostatic tilt, Circulation 90 (4) (1994) 1826–1831, https://doi.org/10.1161/01.cir.90.4.1826.

[16] A. Porta, M. Baumert, D. Cysarz, N. Wessel, Enhancing dynamical signatures of complex systems through symbolic computation, Phil. Trans. R. Soc. A Philos. Trans. A Math. Phys. Eng. Sci. 373 (2034) (2015) 20140099, https://doi.org/10.1098/rsta.2014.0099.

[17] A. Voss, J. Kurths, H.J. Kleiner, A. Witt, N. Wessel, P. Saparin, K.J. Osterziel, R. Schurath, R. Dietz, The application of methods of non-linear dynamics for the improved and predictive recognition of patients threatened by sudden cardiac death, Cardiovasc. Res. 31 (3) (1996) 419–433.

[18] N. Wessel, C. Ziehmann, J. Kurths, U. Meyerfeldt, A. Schirdewan, A. Voss, Short-term forecasting of life-threatening cardiac arrhythmias based on symbolic dynamics and finite-time growth rates, Phys. Rev. E 61 (1) (2000) 733–739, https://doi.org/10.1103/PhysRevE.61.733.

[19] D. Cysarz, H. Bettermann, P. Van Leeuwen, Entropies of short binary sequences in heart period dynamics, Am. J. Physiol. Heart Circ. Physiol. 278 (6) (2000) H2163–H2172, https://doi.org/10.1152/ajpheart.2000.278.6.H2163.

[20] H. Bettermann, D. Cysarz, P. Van Leeuwen, Detecting cardiorespiratory synchronization by respiratory pattern analysis of heart period dynamics: the musical rhythm approach, Int. J. Bifurcat. Chaos 10 (10) (2000) 2349–2360, https://doi.org/10.1142/S021812740000150X.

[21] J.J. Żebrowski, W. Popławska, R. Baranowski, T. Buchner, Symbolic dynamics and complexity in a physiological time series, Chaos Solitons Fractals 11 (7) (2000) 1061–1075, https://doi.org/10.1016/S0960-0779(99)00004-1.

[22] A. Porta, S. Guzzetti, N. Montano, R. Furlan, A. Malliani, S. Cerutti, Entropy, entropy rate and pattern classification as tools to typify complexity in short heart period variability series, IEEE Trans. Biomed. Eng. 48 (11) (2001) 1282–1291, https://doi.org/10.1109/10.959324.

[23] M. Baumert, T. Walther, J. Hopfe, H. Stefan, R. Faber, A. Voss, Joint symbolic dynamics analysis of beat-to-beat interactions of heart rate and systolic blood pressure in normal pregnancy, Med. Biol. Eng. Comput. 40 (2) (2002) 241–246, https://doi.org/10.1007/BF02348131.

[24] A.C. Yang, S.S. Hseu, H.W. Yien, A.L. Goldberger, C.K. Peng, Linguistic analysis of the human heartbeat using frequency and rank order statistics, Phys. Rev. Lett. 90 (10) (2003) 108103, https://doi.org/10.1103/PhysRevLett.90.108103.

[25] S. Guzzetti, E. Borroni, P.E. Garbelli, E. Ceriani, P. Della Bella, N. Montano, C. Cogliati, V. Somers, A. Malliani, A. Porta, Symbolic dynamics of heart rate variability: a probe to investigate cardiac autonomic modulation, Circulation 112 (4) (2005) 465–470, https://doi.org/10.1161/circulationaha.104.518449.

[26] A. Porta, L. Faes, M. Masé, G. D'Addio, G.D. Pinna, R. Maestri, N. Montano, R. Furlan, S. Guzzetti, G. Nollo, A. Malliani, An integrated approach based on uniform quantization for the evaluation of complexity of short-term heart period variability: application to 24h holter recordings in healthy and heart failure humans, Chaos 17 (1) (2007) 015117, https://doi.org/10.1063/1.2404630.

[27] A. Porta, E. Tobaldini, S. Guzzetti, R. Furlan, N. Montano, T. Gnecchi-Ruscone, Assessment of cardiac autonomic modulation during graded head-up tilt by symbolic analysis of heart rate variability, Am. J. Physiol. 293 (1) (2007) H702–H708, https://doi.org/10.1152/ajpheart.00006.2007.

[28] N. Wessel, H. Malberg, R. Bauernschmitt, J. Kurths, Nonlinear methods of cardiovascular physics and their clinical applicability, Int. J. Bifurcat. Chaos 17 (10) (2007) 3325–3371, https://doi.org/10.1142/S0218127407019093.

[29] M.M. Kabir, D.A. Saint, E. Nalivaiko, D. Abbott, A. Voss, M. Baumert, Quantification of cardiorespiratory interactions based on joint symbolic dynamics, Ann. Biomed. Eng. 39 (10) (2011) 2604–2614, https://doi.org/10.1007/s10439-011-0332-3.

[30] D. Cysarz, P. Van Leeuwen, F. Edelhauser, N. Montano, A. Porta, Binary symbolic dynamics classifies heart rate variability patterns linked to autonomic modulations, Comput. Biol. Med. 42 (3) (2012) 313–318, https://doi.org/10.1016/j.compbiomed.2011.04.013.

[31] U. Parlitz, S. Berg, S. Luther, A. Schirdewan, J. Kurths, N. Wessel, Classifying cardiac biosignals using ordinal pattern statistics and symbolic dynamics, Comput. Biol. Med. 42 (3) (2012) 319–327, https://doi.org/10.1016/j.compbiomed.2011.03.017.

[32] M. Baumert, K. Javorka, M.M. Kabir, Joint symbolic dynamics for the assessment of cardiovascular and cardiorespiratory interactions, Philos. Trans. A Math. Phys. Eng. Sci. 373 (2034) (2015) 20140097, https://doi.org/10.1098/rsta.2014.0097.

[33] J.M. Amigó, K. Keller, V.A. Unakafova, Ordinal symbolic analysis and its application to biomedical recordings, Philos. Trans. A Math. Phys. Eng. Sci. 373 (2034) (2015) 20140091, https://doi.org/10.1098/rsta.2014.0091.

[34] A. Porta, A. Marchi, V. Bari, K. Heusser, J. Tank, J. Jordan, F. Barbic, R. Furlan, Conditional symbolic analysis detects non linear influences of respiration on cardiovascular control in humans, Philos. Trans. A Math. Phys. Eng. Sci. 373 (2034) (2015) 20140096, https://doi.org/10.1098/rsta.2014.0096.

[35] D. Cysarz, P. Van Leeuwen, F. Edelhauser, N. Montano, V.K. Somers, A. Porta, Symbolic transformations of heart rate variability preserve information about

cardiac autonomic control, Physiol. Meas. 36 (4) (2015) 643–657, https://doi.org/10.1088/0967-3334/36/4/643.
[36] K. Lehnertz, H. Dickten, Assessing directionality and strength of coupling through symbolic analysis: an application to epilepsy patients, Philos. Trans. A Math. Phys. Eng. Sci. 373 (2034) (2015) 20140094, https://doi.org/10.1098/rsta.2014.0091.
[37] M. Baumert, M. Schmidt, S. Zaunseder, A. Porta, Effects of ECG sampling rate on QT interval variability measurement, Biomed. Signal Process Control 25 (2016) 159–164, https://doi.org/10.1016/j.bspc.2015.11.011.
[38] M.D. Costa, R.B. Davis, A.L. Goldberger, Heart rate fragmentation: a symbolic dynamical approach, Front. Physiol. 8 (2017) 827, https://doi.org/10.3389/fphys.2017.00827.
[39] D. Cysarz, F. Edelhauser, M. Javorka, N. Montano, A. Porta, On the relevance of symbolizing heart rate variability by means of a percentile-based coarse graining approach, Physiol. Meas. 39 (10) (2018) 105010, https://doi.org/10.1088/1361-6579/aae302.
[40] C. Spellenberg, P. Heusser, A. Büssing, A. Savelsbergh, D. C ysarz, Binary symbolic dynamics analysis to detect stress-associated changes of nonstationary heart rate variability, Sci. Rep. 10 (1) (2020) 15440, https://doi.org/10.1038/s41598-020-72034-2.
[41] J.L. Storniolo, B. Cairo, A. Porta, P. Cavallari, Symbolic analysis of the heart rate variability during the plateau phase following maximal sprint exercise, Front. Physiol. 12 (2021) 632883, https://doi.org/10.3389/fphys.2021.632883.
[42] D. Cysarz, A. Porta, N. Montano, P. Van Leeuwen, J. Kurths, Quantifying heart rate dynamics using different approaches of symbolic dynamics, Eur. Phys. J.: Spec. Top. 222 (2013) 487–500, https://doi.org/10.1140/epjst/e2013-01854-7.
[43] A. Porta, V. Bari, B. Cairo, B. De Maria, E. Vaini, F. Barbic, R. Furlan, Comparison of symbolization strategies for complexity assessment of spontaneous variability in individuals with signs of cardiovascular control impairment, Biomed. Signal Process Control 62 (2020) 102128, https://doi.org/10.1016/j.bspc.2020.102128.
[44] J. Parlow, J.-P. Viale, G. Annat, R.L. Hughson, L. Quintin, Spontaneous cardiac baroreflex in humans: comparison with drug-induced responses, Hypertension 25 (5) (1995) 1058–1068, https://doi.org/10.1161/01.hyp.25.5.1058.
[45] E. Toader, A. Cividjian, N. Rentero, R.M. McAllen, L. Quintin, Cardioinhibitory actions of clonidine assessed by cardiac vagal motoneuron recordings, J. Hypertens. 26 (6) (2008) 1169–1180, https://doi.org/10.1097/HJH.0b013e3282fd10e0.
[46] A. Porta, A.M. Catai, A.C.M. Takahashi, V. Magagnin, T. Bassani, E. Tobaldini, P. van de Borne, N. Montano, Causal relationships between heart period and systolic arterial pressure during graded head-up tilt, Am. J. Physiol. Regul. Integr. Comp. Physiol. 300 (2) (2011) R378–R386, https://doi.org/10.1152/ajpregu.00553.2010.
[47] F. Barbic, F. Perego, M. Canesi, M. Gianni, S. Biagiotti, G. Costantino, G. Pezzoli, A. Porta, A. Malliani, R. Furlan, Early abnormalities of vascular and cardiac autonomic control in Parkinson's disease without orthostatic hypotension, Hypertension 49 (1) (2007) 120–126, https://doi.org/10.1161/01.HYP.0000250939.71343.7c.
[48] A. Porta, P. Castiglioni, B. Cairo, V. Bari, B. De Maria, L. Quintin, Symbolic analysis and amplitude symbolic analysis provide complementary information on cardiac control. Computing in Cardiology 2025, São Paulo, Brazil, September .
[49] T. Wu, Y. Tang, K. Aihara, Overcoming feature scarcity in complex system prediction: an alternative delay embedding, Chaos 35 (2025) 083128, https://doi.org/10.1063/5.0279303.
[50] J.G. van Dijk, J. Haan, K. Zwinderman, B. Kremer, B.J. van Hilten, R.A. Roos, Autonomic nervous system dysfunction in Parkinson's disease: relation with age, medication, duration, and severity, J. Neurol. Neurosurg. Psychiatry 56 (10) (1993) 1090–1095, https://doi.org/10.1136/jnnp.56.10.1090.
[51] D.S. Goldstein, Dysautonomia in Parkinson's disease: neurocardiological abnormalities, Lancet Neurol. 2 (11) (2003) 669–676, https://doi.org/10.1016/s1474-4422(03)00555-6.
[52] T. Ziemssen, H. Reichmann, Cardiovascular autonomic dysfunction in Parkinson's disease, J. Neurol. Sci. 289 (1–2) (2010) 74–80, https://doi.org/10.1016/j.jns.2009.08.031.
[53] M. Kallio, T.H. Haapaniemi, J. Turkka, K. Suominen, U. Tolonen, K.A. Sotaniemi, V.-P. Heikkila, V.V. Myllyla, Heart rate variability in patients with untreated Parkinson disease, Eur. J. Neurol. 7 (6) (2000) 667–672, https://doi.org/10.1046/j.1468-1331.2000.00127.x.
[54] T.H. Haapaniemi, V. Pursiainen, J.T. Korpelainen, H.V. Huikuri, K.A. Sotaniemi, V. V. Myllyla, Ambulatory ECG and analysis of heart rate variability in Parkinson's disease, J. Neurol. Neurosurg. Psychiatry 70 (3) (2001) 305–310, https://doi.org/10.1136/jnnp.70.3.305.
[55] D. Linden, R.R. Diehl, P. Berlit, Sympathetic cardiovascular dysfunction in long-standing idiopatic Parkinson's disease, Clin. Auton. Res. 7 (6) (1997) 311–314, https://doi.org/10.1007/BF02267723.
[56] J.-A. Palma, H. Kaufmann, Orthostatic hypotension in Parkinson disease, Clin. Geriatr. Med. 36 (1) (2020) 53–67, https://doi.org/10.1016/j.cger.2019.09.002.
[57] F. Barbic, M. Galli, L. Dalla Vecchia, M. Canesi, V. Cimolin, A. Porta, V. Bari, G. Cerri, F. Dipaola, T. Bassani, D. Cozzolino, G. Pezzoli, R. Furlan, The effects of mechanical stimulation of the feet on gait and cardiovascular autonomic control in Parkinson's disease, J. Appl. Physiol. 116 (5) (1985) 495–503, https://doi.org/10.1152/japplphysiol.01160.2013, 2014.
[58] D.S. Goldstein, C.S. Holmes, R. Dendi, S.R. Bruce, S.T. Li, Orthostatic hypotension from sympathetic denervation in Parkinson's disease, Neurology 58 (8) (2002) 1247–1255, https://doi.org/10.1212/wnl.58.8.1247.
[59] J. Cernanova Krohova, J. Oleksakova, Z. Turianikova, B. Czippelova, M. Grofik, E. Kurca, M. Javorka, Early parasympathetic dysfunction in Parkinson's disease: insights from information-theoretic analysis, Front. Netw. Physiol. 5 (2025) 1680069, https://doi.org/10.3389/fnetp.2025.1680069.
[60] T. Bassani, V. Bari, A. Marchi, S. Tassin, L. Dalla Vecchia, M. Canesi, F. Barbic, R. Furlan, A. Porta, Model-free causality analysis of cardiovascular variability detects the amelioration of the autonomic control in Parkinson's disease patients undergoing mechanical stimulation, Physiol. Meas. 35 (2014) 1397–1408, https://doi.org/10.1088/0967-3334/35/7/1397.
[61] V. Magagnin, T. Bassani, V. Bari, M. Turiel, R. Maestri, G.D. Pinna, A. Porta, Non-stationarities significantly distort short-term spectral, symbolic and entropy heart rate variability indexes, Physiol. Meas. 32 (11) (2011) 1775–1786, https://doi.org/10.1088/0967-3334/32/11/S05.